AAS 17-747

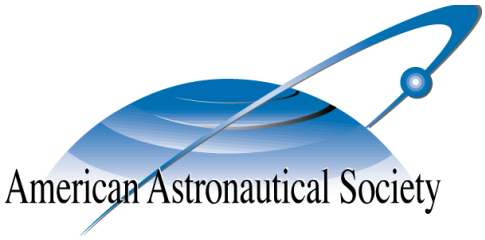

American Institute of
Aeronautics and Astronautics

DYNAMIC MODELING OF FOLDED DEPLOYABLE SPACE STRUCTURES WITH FLEXIBLE HINGES

JoAnna Fulton and Hanspeter Schaub

AAS/AIAA Astrodynamics Specialist Conference

Stevenson, Washington August 20–24, 2017

AAS Publications Office, P.O. Box 28130, San Diego, CA 92198

AAS 17-747

DYNAMIC MODELING OF FOLDED DEPLOYABLE SPACE STRUCTURES WITH FLEXIBLE HINGES

JoAnna Fulton* **and Hanspeter Schaub†**

A modeling approach for capturing the three-dimensional deployment dynamics of complex folded deployable structures with flexible hinges on spacecraft is developed. This paper provides an initial investigation on how to model flexible hinges that connect rigid panels. Such hinges are emerging as a promising use of composite materials to create novel folded structures. The nonlinear multi-body dynamics is studied and described using an energy-based approach and parameterizations developed for attitude dynamics and control to better understand how the structure's motion affects the spacecraft. While this study assumes a simple hinge-response behavior, the dynamical formulation is general enough to substitute experimentally derived response functions in future efforts.

INTRODUCTION

This paper aims to develop a modeling technique to capture the deployment dynamics of complex folded deployable space structures on spacecraft. Folded deployable space structures are a class of structures where the surface is segmented by a given pattern to be compactly folded. These structures are a promising concept to address a growing need in deployable structures technology. Several contemporary mission concepts require structures on the order of 10s or 100s of meters diameter in size, far exceeding the 5 meter diameter constraint of launch vehicle fairings.[1] For example, the free-flying occulter concept for exoplanet imaging missions such as THEIA and New Worlds Observer[2] has a structure diameter of 40 meters at minimum.[3] It's acknowledged that deployables are critical for future astrophysics missions,[4] as has already been demonstrated with the James Webb Space Telescope architecture and the proposed High Definition Space Telescope. Future manned missions using solar electric propulsion will rely on solar power production at scales requiring massive deployable solar panel systems. For these examples, a continuous rigid or semi-rigid surface structure is required, such that sparse structure architectures such as mesh or membrane structures are not applicable, but foldable concepts work well. Additionally, this work not only applies to large structures, but is also critical to small spacecraft where the deployed structure is much larger than the bus size.

For cases where the deployed structure is several factors greater in size than the spacecraft bus, the dynamics of the deployment and the effect on the host bus dynamics are of significant concern. The current approach in the field relies on experimental testing and Finite Element Analysis (FEA)

*Graduate Research Assistant, Aerospace Engineering Sciences, University of Colorado at Boulder, 431 UCB, Colorado Center for Astrodynamics Research, Boulder, CO 80309-0431

†Alfred T. and Betty E. Look Professor of Engineering, Aerospace Engineering Sciences, University of Colorado at Boulder, 431 UCB, Colorado Center for Astrodynamics Research, Boulder, CO 80309-0431

software to verify deployment for developing structure designs, a slow and resource expensive process. Additionally, novel concepts for folded space structures use highly flexible materials for hinge connections across folds. These materials enable significant mass savings and are able to actuate the deployment through strain energy alone. However, the behavior of these materials are difficult to model using FEA tools, and modeling a system with many hinges acting simultaneously is highly computationally expensive.

Modeling the dynamics of deployable structure and spacecraft systems using a more efficient approach has not been investigated due to the complexity and lack of approach precedence in the literature. The deployment dynamics of complex deployable systems must be understood to verify deployment and to ensure mission success, and should be available early in the design process to enable more efficient and reliable designs. In this paper, modeling the hinge behaviors in folded deployable structures as functions of the translational and rotational displacement is investigated. This approach is applied to a prototypical single panel and a three panel folded structure pattern. The system is studied and described using dynamics techniques traditionally developed for attitude dynamics and control to better understand how the structure's motion affects the spacecraft motion.

OVERVIEW OF ORIGAMI-INSPIRED FOLDING SPACE STRUCTURES

A prevalent concept for designing folding structures has drawn inspiration from origami folding techniques. Many fold patterns are developed for two dimensional surfaces, such as the Miura-Ori, the Scheel pattern,[5] and others.[6] Fold patterns are being extensively studied for space applications in the field of flexible gossamer membrane space structures,[7,8] and are applied to solar sails,[9,10] defractive optics,[11] and many more concepts.[12] However these studies in highly lightweight membrane technologies are primarily focused on feasibility, concept demonstration, and stiffness analysis, and do not delve deeply into deployment dynamics or system dynamics modeling. Additionally, these structures are less concerned about dynamic effects due to the properties of lightweight membrane materials and due to the smaller size scale of these designs. Concepts concerning rigid or semi-rigid plate folding structures that mimic the fold patterns of these membrane structures are also being considered,[13] and for these concepts, the dynamics can no longer be neglected.

A folded planar surface is referred to here and in the literature as a "flasher". The fold patterns applied to the these space structure flashers have common characteristics. The first is in the orientation of the folded state with respect to the spacecraft bus. The most effective folding designs for circular and symmetric structures such as occulting disks, antenna, and optics have a radially oriented pattern, that either wraps about the hub or collapses circumferentially into the hub. An example of this concept is illustrated in Figure 1. Radial patterns enable the design to maintain symmetric inertia properties, a highly desired characteristic for any spacecraft, and allow the structure to be stowed on the perimeter. In this paper, radial patterns will be the primary motivation, however the modeling techniques developed here might also be adapted to map-pattern folded flashers. While radially wrapped folded structures are advantageous, the deployment of such configurations requires that the structure spin away from the hub. The momentum balance of such a system results in a spin rate differential between the hub and the structure that can be problematic at the moment of full deployment. Without control, this can cause re-wrapping and other issues.[14] This study aims to capture this behavior through the dynamics models.

A primary challenge for folded space structures is determining advantageous methods to actuate deployment. One such method focuses on hinge designs and materials where energy is stored in the hinge and actuates deployment on release. Mechanical hinges, compliant mechanisms, and steel

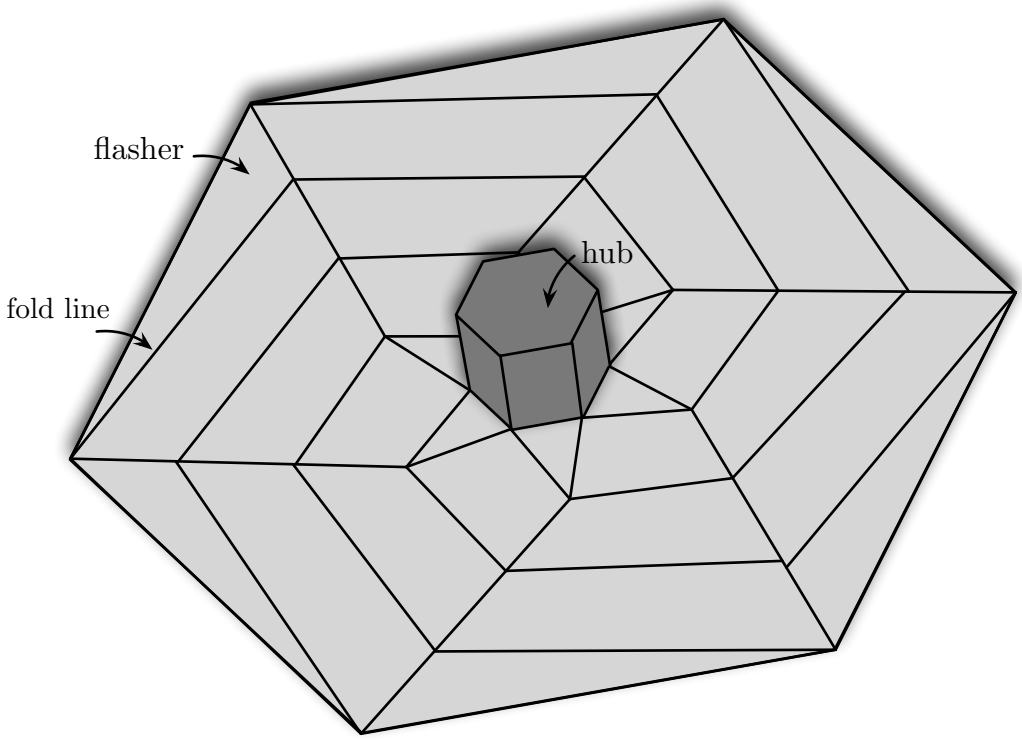

Figure 1. A simple deployed flasher example illustrating the base folds of the Scheel pattern.

tape spring hinges have been studied in the past for this. Additionally, recent investigations in deployable structure materials have focused on the development of highly flexible composite materials for a wide variety of uses, including as hinges for folded structures.[15] These composite materials are desirable due to their lightweight properties and strain energy behavior. These flexible hinges are not necessarily constrained, single rotation hinges however, and complex three dimensional fold capabilities have been demonstrated on tape spring hinges.[16] Figure 2 displays basic diagrams of tape spring configurations, where an ideal simple rotational fold is one degree of freedom, however these flexible materials are capable of multiple axis rotations that do not occur at the hinge midpoint. This paper focuses on the basic modeling of such hinged systems, and how they should be kinematically described relative to a generally rotating rigid spacecraft hub. The scope of this paper assumes relatively simple hinge force and torque response function. The dynamical formulation, however, is setup generally enough that more complex hinge response behaviors can readily be substituted in future work.

MODELING APPROACH

A simple example of a folded space structure is a z-folded solar array, where the fold pattern extends the structure linearly through single axis rotations. For the applications mentioned above, more complex patterns are needed, where panels are folded on multiple edges and undergo full three dimensional rotations through the fold. Therefore, these problems must be approached using

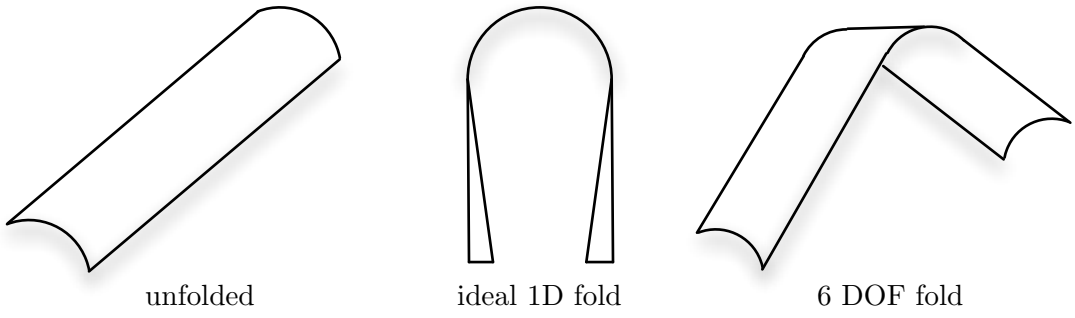

Figure 2. Tape spring hinges are simple, lightweight hinge solutions capable of many fold configurations.

full three dimensional rotational and translational descriptions, and will not be simplified to single degree of freedom kinematic chains. Additionally, the coupling of the panel behaviors and the spacecraft attitude are of primary concern. Therefore, intuitive relations between the panel descriptions and the hub descriptions are pursued. The modeling approach is developed using energy-based dynamics modeling methods, particularly Lagrange's Equations, to create full multi-body dynamics models. This method works well for derivations of n-body problems such as this, where energy can be described in general coordinates for each panel set. The equations of motion as found through Lagrange's Equation is expressed generally as

$$\frac{\partial}{\partial t}\frac{\partial T}{\partial \dot{q}_i} - \frac{\partial T}{\partial q_i} = Q_i \tag{1}$$

where Q_i is the generalized force and can represent conservative and non-conservative forces and torques, T is the kinetic energy of the system, and q_i are the generalized coordinates. There are many ways to describe these three components, and the formulation will become less trivial as the model expands across larger structure flashers. The generalized coordinates of each rigid sub-component contains 6 degrees of freedom, which are best described in either global position and orientations or relative position and orientations. The trade here is due to kinetic energy being a function of global terms, and the generalized forces being a function of the relative terms. The definition of the relative terms, $\boldsymbol{\delta}_{\mathcal{A}/\mathcal{A}_0}$ and $\boldsymbol{\theta}_{\mathcal{A}/\mathcal{A}_0}$, are illustrated in Figure 3 on a single panel example. The body-fixed $\mathcal{A}_0$ frame represents the position and orientation at which there are no restorative forces or torques acting between the two bodies. The panel-fixed $\mathcal{A}$ frame represents the actual position and orientation of the panel relative to this reference, and when these two frames are aligned, there are no internal hinge forces or torques in the system.

In this approach, the relative term descriptions are needed for integrating empirical models of flexible hinge behaviors into the multi-body dynamics simulation. Experiments on hinge force and torque responses can be conducted on a single hinge test article for all possible combinations of displacement and orientation. A mathematical approximation of the hinge behavior as a function of the relative coordinates would be ideal, however even without a mathematical fit, a interpolation over a look up table would also provide this. Therefore, the generalized forces are written in terms of the relative position displacement and relative orientation of the attached panel. All forces are modeled as generalized forces Q_i, instead of using potential functions, as this study is interested

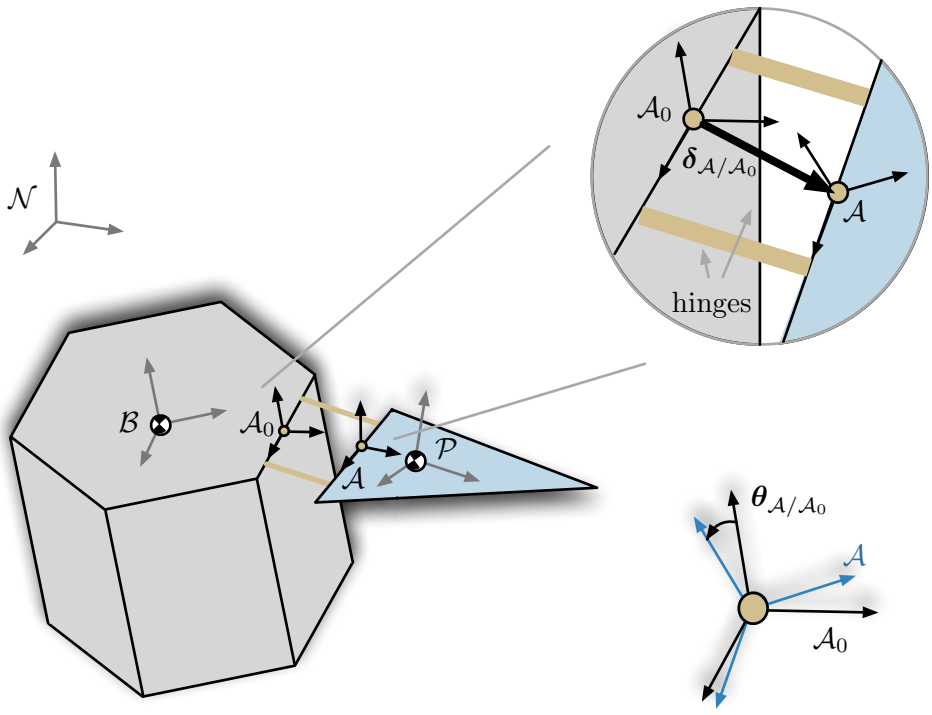

Figure 3. Reference frame and relative coordinate definitions of one panel.

in developing a framework where any forces written as functions of the hinge displacement and orientation relative to the body can be applied.

SPACECRAFT BUS AND SINGLE PANEL MODEL DERIVATION

Equations of Motion Development

A single panel case is first considered to develop the hinge representation expressions. This case is set up as two general bodies representing a spacecraft bus and a rigid panel. The spacecraft bus center of mass position, $\boldsymbol{R}_{\mathcal{B}/\mathcal{N}}$, and orientation, $\boldsymbol{\theta}_{\mathcal{B}/\mathcal{N}}$, are unconstrained and tracked through inertial space. For this study the body orientation is parameterized using 3-2-1 Euler Angles, but any attitude parameterization can be applied. The spacecraft bus kinetic energy is then determined through

$$T_B = \frac{1}{2}\boldsymbol{\omega}_{\mathcal{B}/\mathcal{N}}[I_{\mathcal{B}}]\boldsymbol{\omega}_{\mathcal{B}/\mathcal{N}} + \frac{1}{2}m_B\dot{\boldsymbol{R}}_{\mathcal{B}/\mathcal{N}} \cdot \dot{\boldsymbol{R}}_{\mathcal{B}/\mathcal{N}} \tag{2}$$

Where the $\mathcal{B}$ frame is a body fixed frame and $\mathcal{N}$ indicates an inertial frame. A diagram of the required reference frames is shown in Figure 3. Additionally, $\boldsymbol{\omega}_{\mathcal{B}/\mathcal{N}}$ is the rotation rate of the body with respect to the inertial frame, $[I_B]$ is the body inertia tensor, m_B is the body mass, and $\dot{\boldsymbol{R}}_{\mathcal{B}/\mathcal{N}}$ is the inertial velocity of the body. Similarly, the kinetic energy of the panel is written in a general form, for a panel fixed frame $\mathcal{P}$, as

$$T_P = \frac{1}{2}\boldsymbol{\omega}_{\mathcal{P}/\mathcal{N}}[I_P]\boldsymbol{\omega}_{\mathcal{P}/\mathcal{N}} + \frac{1}{2}m_P\dot{\boldsymbol{R}}_{\mathcal{P}/\mathcal{N}} \cdot \dot{\boldsymbol{R}}_{\mathcal{P}/\mathcal{N}} \tag{3}$$

Where $\boldsymbol{\omega}_{\mathcal{P}/\mathcal{N}}$ is the rotation rate of the panel with respect to the inertial frame, $[I_P]$ is the panel inertia tensor, m_P is the panel mass, and $\dot{\boldsymbol{R}}_{\mathcal{P}/\mathcal{N}}$ is the inertial velocity of the panel.

Then the total kinetic energy of the system is the sum of these two contributions. The generalized coordinates are selected to include the spacecraft states as expressed in the spacecraft body frame, and the panel relative coordinates as expressed in the zero-orientation $\mathcal{A}_0$ frame,

$$\boldsymbol{q} = \begin{bmatrix} {}^{\mathcal{B}}\boldsymbol{R}_{\mathcal{B}/\mathcal{N}} & {}^{\mathcal{B}}\boldsymbol{\theta}_{\mathcal{B}/\mathcal{N}} & {}^{\mathcal{A}_0}\boldsymbol{\delta}_{\mathcal{A}/\mathcal{A}_0} & {}^{\mathcal{A}_0}\boldsymbol{\theta}_{\mathcal{A}/\mathcal{A}_0} \end{bmatrix}^{\mathsf{T}} \tag{4}$$

Where the inertial position of the panel is

$$\boldsymbol{R}_{\mathcal{P}/\mathcal{N}} = \boldsymbol{r}_{\mathcal{P}/\mathcal{A}} + \boldsymbol{\delta}_{\mathcal{A}/\mathcal{A}_0} + \boldsymbol{r}_{\mathcal{A}_0/\mathcal{B}} + \boldsymbol{R}_{\mathcal{B}/\mathcal{N}} \tag{5}$$

the inertial velocity is determined using the transport theorem,[17] where each position vector is expressed in a convenient frame. The inertial velocity is a function of the position and the rate of the frame it is expressed in with respect to the inertial frame. This presents the need for careful frame selection and expression. To develop the most general solution, each vector will be expressed in the spacecraft body frame. Then the velocity expression is

$$\dot{\boldsymbol{R}}_{\mathcal{P}/\mathcal{N}} = \frac{{}^{\mathcal{B}}\mathrm{d}}{\mathrm{d}t}\left(\boldsymbol{r}_{\mathcal{P}/\mathcal{A}} + \boldsymbol{\delta}_{\mathcal{A}/\mathcal{A}_0} + \boldsymbol{R}_{\mathcal{B}/\mathcal{N}}\right) + \boldsymbol{\omega}_{\mathcal{B}/\mathcal{N}} \times \boldsymbol{R}_{\mathcal{P}/\mathcal{N}} \tag{6}$$

To express each relative position vector in the body frame, the transformation of the vector's expressed frame to the body frame is needed. The relative orientation of the hinge attachment frames, the $\mathcal{A}$ and $\mathcal{A}_0$ frames, to their fixed bodies, the $\mathcal{P}$ and $\mathcal{B}$ frames respectively, are defined for any general configuration and recorded as 3-2-1 Euler Angles. This allows flexibility in the system assembly and keeps the analysis applicable to all panel shapes and configurations. The relative orientation between each frame is then converted to corresponding direction cosine matrices. The frames are illustrated in Figure 3, and because the $\mathcal{A}_0$ frame is fixed in the $\mathcal{B}$ frame, the orientation is time invariant. Similarly, the orientation of the attachment origin on the panel frame relative to the panel, $\mathcal{A}$, is time invariant. Then the relative orientations are

$$[\mathcal{P}\mathcal{A}] = f(\theta_{1,\mathcal{P}/\mathcal{A}}, \theta_{2,\mathcal{P}/\mathcal{A}}, \theta_{3,\mathcal{P}/\mathcal{A}}) \tag{7a}$$

$$[\mathcal{B}\mathcal{A}_0] = f(\theta_{1,\mathcal{B}/\mathcal{A}_0}, \theta_{2,\mathcal{B}/\mathcal{A}_0}, \theta_{3,\mathcal{B}/\mathcal{A}_0}) \tag{7b}$$

Additionally, the transformations of the generalized orientations are

$$[\mathcal{A}\mathcal{A}_0] = f(\theta_{1,\mathcal{A}/\mathcal{A}_0}(t), \theta_{2,\mathcal{A}/\mathcal{A}_0}(t), \theta_{3,\mathcal{A}\mathcal{A}_0}(t)) \tag{8a}$$

$$[\mathcal{B}\mathcal{N}] = f(\theta_{1,\mathcal{B}\mathcal{N}}(t), \theta_{2,\mathcal{B}\mathcal{N}}(t), \theta_{3,\mathcal{B}\mathcal{N}}(t)) \tag{8b}$$

The relative orientation between the $\mathcal{P}$ and $\mathcal{N}$ frames are determined then from direction cosine matrices as

$$[\mathcal{P}\mathcal{N}] = [\mathcal{P}\mathcal{A}][\mathcal{A}\mathcal{A}_0][\mathcal{B}\mathcal{A}_0]^{\mathsf{T}}[\mathcal{B}\mathcal{N}] \tag{9}$$

This orientation matrix models how the panel rotates relative to the inertial frame and is needed to express the panel inertial rate in the kinetic energy function, where the kinematic differential equation of this orientation is known for 3-2-1 Euler Angles.[17] This attitude is highly nonlinear expression as a function of the time variant general coordinates $\boldsymbol{\theta}_{\mathcal{B}/\mathcal{N}}(t)$ and $\boldsymbol{\theta}_{\mathcal{A}/\mathcal{A}_0}(t)$, as well as the offset orientations $[\mathcal{A}\mathcal{P}]$ and $[\mathcal{B}\mathcal{A}_0]$.

Elastic Hinge Force and Torque Derivation

Now the interactions between these two bodies are to be defined, where the two bodies interact only through the elastic hinge connection. The contributions from elastic hinges are implemented as restorative forces and torques as a function of the relative displacements and rotations between the two bodies. To do this, a relative equilibrium state is defined such that when the bodies reach this state, there are no internal forces or torques acting between the bodies. In this study, these forcing functions are generic place holder representations, however in future studies, these will be replaced with functions that are determined empirically for a given hinge material. The relative states are tracked through two reference frames, an equilibrium frame, $\mathcal{A}_0$, at which zero force and torque is experienced, and a true position frame, $\mathcal{A}$, as depicted in Figure 3. The equilibrium frame is fixed in the body frame, however it does not share the same position or orientation as the body center of mass because these forces and torques are not acting directly at the body center of mass. Conversely, the relative position frame is fixed in the panel frame.

Here a derivation of the relative force and torque between two bodies is presented. The classical definition for N generalized forces Q_j is[17,18]

$$Q_j = \sum_{i=1}^{N} \boldsymbol{f}_i \cdot \frac{\partial \boldsymbol{R}_i}{\partial q_j} \tag{10}$$

where $\boldsymbol{R}_i$ is the location of the point where the force is being applied. The generalized force expression of a pure inertial torque, $\boldsymbol{L}$ acting on an arbitrary body $\mathcal{E}$, is derived from this as[17]

$$Q_j = \boldsymbol{\tau} \cdot \frac{\partial \boldsymbol{\omega}_{\mathcal{E}/\mathcal{N}}}{\partial \dot{q}_j} \tag{11}$$

The internal restorative force and torque of the hinge will act in equal and opposite sense on the bus and panel, however, they will not be acting on the same locations in inertial space due to the displacement of the hinge. Therefore these force and torque vectors are expressed in general coordinates as follows

$$Q_j = \boldsymbol{F}_{\mathcal{A}/\mathcal{A}_0} \cdot \frac{\partial \boldsymbol{R}_{\mathcal{A}_0/\mathcal{N}}}{\partial q_j} - \boldsymbol{F}_{\mathcal{A}/\mathcal{A}_0} \cdot \frac{\partial \boldsymbol{R}_{\mathcal{A}/\mathcal{N}}}{\partial q_j} + \boldsymbol{\tau}_{\mathcal{A}/\mathcal{A}_0} \cdot \frac{\partial \boldsymbol{\omega}_{\mathcal{A}_0/\mathcal{N}}}{\partial \dot{q}_j} - \boldsymbol{\tau}_{\mathcal{A}/\mathcal{A}_0} \cdot \frac{\partial \boldsymbol{\omega}_{\mathcal{A}/\mathcal{N}}}{\partial \dot{q}_j} \tag{12}$$

Recognizing that the bus and panel are each rigid bodies and expanding yields

$$\begin{aligned} Q_j = \boldsymbol{F}_{\mathcal{A}/\mathcal{A}_0} \cdot \frac{\partial \boldsymbol{R}_{\mathcal{A}_0/\mathcal{N}}}{\partial q_j} - \boldsymbol{F}_{\mathcal{A}/\mathcal{A}_0} \cdot \frac{\partial (\boldsymbol{\delta}_{\mathcal{A}_0/\mathcal{A}} + \boldsymbol{R}_{\mathcal{A}_0/\mathcal{N}})}{\partial q_j} \\ + \boldsymbol{\tau}_{\mathcal{A}/\mathcal{A}_0} \cdot \frac{\partial \boldsymbol{\omega}_{\mathcal{B}/\mathcal{N}}}{\partial \dot{q}_j} - \boldsymbol{\tau}_{\mathcal{A}/\mathcal{A}_0} \cdot \frac{(\partial \boldsymbol{\omega}_{\mathcal{A}/\mathcal{A}_0} + \partial \boldsymbol{\omega}_{\mathcal{B}/\mathcal{N}})}{\partial \dot{q}_j} \end{aligned} \tag{13}$$

Simplifying, the positions and rates relative to inertial cancel out to the following expression

$$Q_j = -\boldsymbol{F}_{\mathcal{A}/\mathcal{A}_0}(\boldsymbol{\delta}_{\mathcal{A}_0/\mathcal{A}}(t)) \cdot \frac{\partial \boldsymbol{\delta}_{\mathcal{A}_0/\mathcal{A}}(t)}{\partial q_j} - \boldsymbol{\tau}_{\mathcal{A}/\mathcal{A}_0}(\boldsymbol{\theta}_{\mathcal{A}/\mathcal{A}_0}(t)) \cdot \frac{\partial \boldsymbol{\omega}_{\mathcal{A}/\mathcal{A}_0}(\boldsymbol{\theta}_{\mathcal{A}/\mathcal{A}_0}(t))}{\partial \dot{q}_j} \tag{14}$$

This reduction reveals that the generalized forces can be expressed as a function of the relative displacement and relative orientation only, a desirable simplification. Finally, the force and torque

expressions must be defined. For this study, the forces and torques are written as linear spring functions for the sake of simplicity of verification.

$$\boldsymbol{F} = [K_F]\boldsymbol{\delta}_{\mathcal{A}/\mathcal{A}_0}(t) \tag{15a}$$

$$\boldsymbol{\tau} = [K_\theta]\begin{bmatrix}\theta_{3,\mathcal{A}/\mathcal{A}_0}(t) & \theta_{2,\mathcal{A}/\mathcal{A}_0}(t) & \theta_{1,\mathcal{A}/\mathcal{A}_0}(t)\end{bmatrix}^\mathsf{T} \tag{15b}$$

An advantage to building the hinge model using this approach is the ability to tune these forcing functions to investigate desired behaviors. For example, a major desire for deployment dynamics is damping the motion to achieve rest at full deployment, avoiding kickback and energy dissipation through undesirable material deformations. By including a damping term in this expression, the required damping properties of a material or device can be investigated. Additionally, in cases where a given motion is negligible, constraint forces can be used to arrest the motion in the simulation.

SPACECRAFT BUS AND SINGLE PANEL MODEL INITIALIZATION AND VALIDATION

The derivation discussed above is carried out using symbolic tools in Mathematica to auto-generate the equations of motion. The script is written in a general way, such that only the spacecraft and panel mass, inertia, and configuration properties are needed to generate a model. Additionally, the model is verified using numerical tools in Mathematica, where only the state initial conditions are required for the simulation. Generation of the generalized forces is also built in a general way, such that any internal hinge force and torque functions can be given to the system.

Knowledge of the spacecraft bus and rigid panel mass and inertia properties is needed, as well as the reference frame configurations in the zero-force orientation. This information is generated here for a simple model in Table 1 and Table 2. Additionally, general initial conditions are generated for this simulation to test the model's performance across all generalized coordinates and are reported in Table 3. However, in a real deployment test scenario, these initial conditions would be generated to simulate the deployable structure's stowed configuration and would be entirely dependent on the kinematic behavior of the flasher pattern and on constraints of the hinge and panel materials.

Table 1. Mass and principle inertia parameters of the single panel simulation.

m_B (kg)	m_P (kg)	I_B (kg/m^2)	I_P (kg/m^2)
100	10	$[100, 100, 100]$	$[1, 1, 1]$

Table 2. Relative positions and orientations of the single panel simulation.

$\boldsymbol{r}_{\mathcal{A}_0/\mathcal{B}}$	$\boldsymbol{\theta}_{\mathcal{A}_0/\mathcal{B}}$	$\boldsymbol{r}_{\mathcal{P}/\mathcal{A}}$	$\boldsymbol{\theta}_{\mathcal{P}/\mathcal{A}}$
$[0.75, 0.433, 0]$ m	$[0, 0, 30]$ deg	$[1, 1, 0]$ m	$[0, 0, 0]$ deg

Table 3. Initial conditions of the single panel simulation.

$\boldsymbol{R}_{\mathcal{B}/\mathcal{N}}(0)$	$\boldsymbol{\theta}_{\mathcal{B}/\mathcal{N}}(0)$	$\boldsymbol{\delta}(0)$	$\boldsymbol{\theta}_{\mathcal{P}/\mathcal{N}}(0)$
$\mathbf{0}$	$\mathbf{0}$	$[1, 1, 1]$ cm	$[10, 20, 30]$ deg

The results of a verification simulation run are displayed in Figure 4. The angular momentum is observed to maintain an effective zero momentum, indicating that the forces and torques act

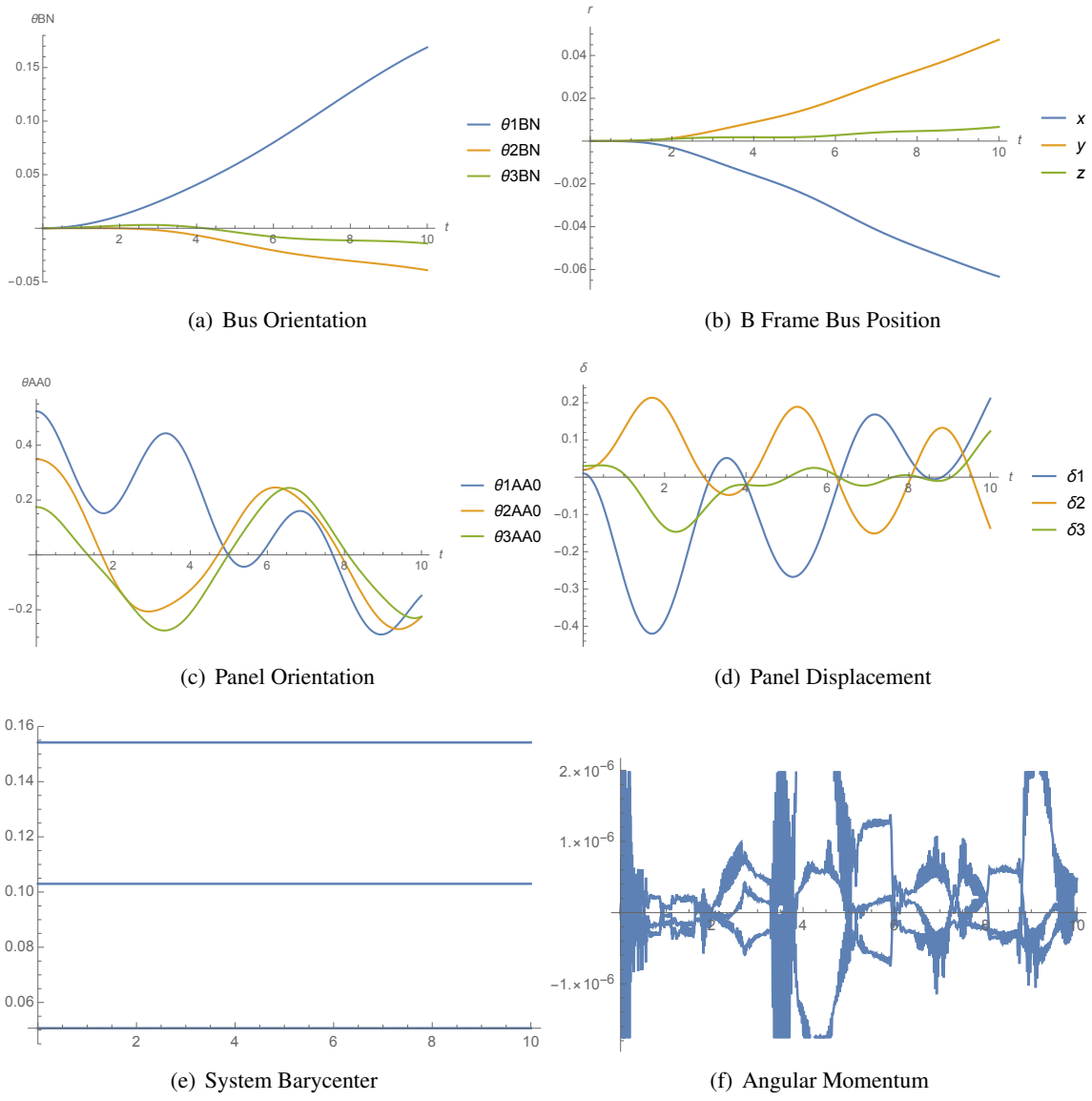

(a) Bus Orientation

(b) B Frame Bus Position

(c) Panel Orientation

(d) Panel Displacement

(e) System Barycenter

(f) Angular Momentum

Figure 4. Single panel simulation results and validations.

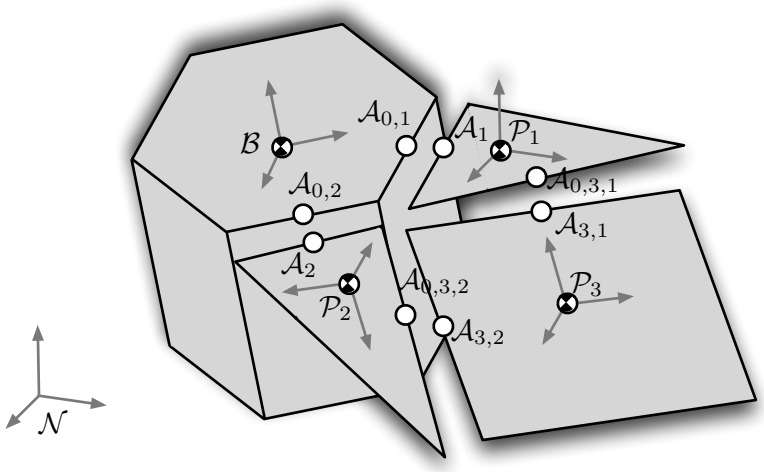

Figure 5. Reference frame definitions of a 3 panel case.

internally and only produce relative motion. This is further verified by tracking the barycenter of the bus and panel system and observing that it maintains a constant position through the simulation, indicating all forces and torques act internally.

MULTIPLE PANEL SET MODEL

Equations of Motion Development

The approach outlined for the single panel case are now expanded to a 4-body, 3-panel case with panel-to-panel interconnections. The derivation for this case is written as generally as possible, where further extrapolation to greater sets of panels would be carried out using the same approach. The model is limited to 3 panels to maintain traceability for the reader. For any N panels, the total kinetic energy of the system is written as

$$T = \frac{1}{2}\boldsymbol{\omega}_{\mathcal{B}/\mathcal{N}}[I_{\mathcal{B}}]\boldsymbol{\omega}_{\mathcal{B}/\mathcal{N}} + \frac{1}{2}m_B\dot{\boldsymbol{R}}_{\mathcal{B}/\mathcal{N}}\cdot\dot{\boldsymbol{R}}_{\mathcal{B}/\mathcal{N}} + \sum_{i=1}^{N}\left[\frac{1}{2}\boldsymbol{\omega}_{\mathcal{P}_i/\mathcal{N}}[I_{\mathcal{P}_i}]\boldsymbol{\omega}_{\mathcal{P}_i/\mathcal{N}} + \frac{1}{2}m_{P_i}\dot{\boldsymbol{R}}_{\mathcal{P}_i/\mathcal{N}}\cdot\dot{\boldsymbol{R}}_{\mathcal{P}_i/\mathcal{N}}\right] \tag{16}$$

The relative generalized coordinates will be selected for this model to simplify identifying desired initial conditions and the zero force and torque configurations. Therefore the generalize coordinates are

$$\boldsymbol{q} = \begin{bmatrix} {}^{\mathcal{B}}\boldsymbol{R}_{\mathcal{B}/\mathcal{N}} & {}^{\mathcal{B}}\boldsymbol{\theta}_{\mathcal{B}/\mathcal{N}} & {}^{\mathcal{A}_{0,1}}\boldsymbol{\delta}_{\mathcal{A}_1/\mathcal{A}_{0,1}} & {}^{\mathcal{A}_{0,1}}\boldsymbol{\theta}_{\mathcal{A}_1/\mathcal{A}_{0,1}} & {}^{\mathcal{A}_{0,2}}\boldsymbol{\delta}_{\mathcal{A}_2/\mathcal{A}_{0,2}} \\ {}^{\mathcal{A}_{0,2}}\boldsymbol{\theta}_{\mathcal{A}_2/\mathcal{A}_{0,2}} & {}^{\mathcal{A}_{0,3,1}}\boldsymbol{\delta}_{\mathcal{A}_{0,3,1}/\mathcal{A}_{3,1}} & {}^{\mathcal{A}_{0,3,1}}\boldsymbol{\theta}_{\mathcal{A}_{0,3,1}/\mathcal{A}_{3,1}} \end{bmatrix}^{\mathsf{T}} \tag{17}$$

Then the inertial position of each panel will have dependencies on the relative position of itself and any connecting panels. For panels adjacent to the body, or in this example, for i = 1,2

$$\boldsymbol{R}_{\mathcal{P}_i/\mathcal{N}} = \boldsymbol{r}_{\mathcal{P}_i/\mathcal{A}_i} + \boldsymbol{\delta}_{\mathcal{A}_i/\mathcal{A}_{0,i}} + \boldsymbol{r}_{\mathcal{A}_{0,i}/\mathcal{B}} + \boldsymbol{R}_{\mathcal{B}/\mathcal{N}} \tag{18}$$

The inertial position vector of the 3rd panel is

$$\boldsymbol{R}_{\mathcal{P}_3/\mathcal{N}} = \boldsymbol{r}_{\mathcal{P}_3/\mathcal{A}_{3,1}} + \boldsymbol{\delta}_{\mathcal{A}_{3,1}/\mathcal{A}_{0,3,1}} + \boldsymbol{r}_{\mathcal{P}_1/\mathcal{A}_1} + \boldsymbol{\delta}_{\mathcal{A}_1/\mathcal{A}_{0,1}} + \boldsymbol{r}_{\mathcal{A}_{0,1}/\mathcal{B}} + \boldsymbol{R}_{\mathcal{B}/\mathcal{N}} \tag{19}$$

Again, the inertial velocity of each panel body is determined using the transport theorem,[17] where multiple reference frames are now in use. The frames for expression of these position descriptions are chosen to simplify these calculations, however it is not possible to avoid a resulting expression that is heavily non-linear and coupled across the generalized coordinates.

Generalized Forces for Multiple Panel Connections

The interdependence of the third panel is observed in Figure 5 where displacement and orientation of the panel must be known with respect to the two adjacent panels. However, the generalized coordinates selected only track one of these relative states to avoid a redundant and over-constrained system. Therefore, the other relative state must be backed out through the kinematic chain as follows, coupling the motion to the adjacent panel.

$$\boldsymbol{\delta}_{\mathcal{A}_{0,3,2}/\mathcal{A}_{3,2}} = (\boldsymbol{r}_{\mathcal{A}_{0,3,2}/\mathcal{P}_2} + \boldsymbol{R}_{\mathcal{P}_2/\mathcal{N}}) - (\boldsymbol{R}_{\mathcal{P}_3/\mathcal{N}} - \boldsymbol{r}_{\mathcal{P}_3/\mathcal{A}_{3,2}}) \tag{20}$$

Additionally, the rotation rates of the third panel with respect to the second must be calculated from the rates of the adjacent bodies

$$\boldsymbol{\omega}_{\mathcal{A}_{0,3,2}/\mathcal{A}_{3,2}} = \boldsymbol{\omega}_{\mathcal{A}_{0,2}/\mathcal{A}_2} - (\boldsymbol{\omega}_{\mathcal{A}_{0,1}/\mathcal{A}_1} + \boldsymbol{\omega}_{\mathcal{A}_{0,3,1}/\mathcal{A}_{3,1}}) \tag{21}$$

With these two additional relationships, the generalized forces and torques can be determined. The simplification found in Equation 14 be used for the force and torque of each hinge, where the generalized forces acting on the system are the sum of the generalized forces generated by each hinge. The total generalized force expression for the system is the sum of these body forces and torques across the system.

$$\begin{aligned}
Q_j = &-\boldsymbol{F}_{\mathcal{B}/\mathcal{P}_1}(\boldsymbol{\delta}_{\mathcal{A}_{0,1}/\mathcal{A}_1}(t)) \cdot \frac{\partial \boldsymbol{\delta}_{\mathcal{A}_{0,1}/\mathcal{A}_1}(t)}{\partial q_j} - \boldsymbol{\tau}_{\mathcal{B}/\mathcal{P}_1}(\boldsymbol{\theta}_{\mathcal{A}_{0,1}/\mathcal{A}_1}(t)) \cdot \frac{\partial \boldsymbol{\omega}_{\mathcal{A}_{0,1}/\mathcal{A}_1}(\boldsymbol{\theta}_{\mathcal{A}_{0,1}/\mathcal{A}_1}(t))}{\partial \dot{q}_j} \\
&- \boldsymbol{F}_{\mathcal{B}/\mathcal{P}_2}(\boldsymbol{\delta}_{\mathcal{A}_{0,2}/\mathcal{A}_2}(t)) \cdot \frac{\partial \boldsymbol{\delta}_{\mathcal{A}_{0,2}/\mathcal{A}_2}(t)}{\partial q_j} - \boldsymbol{\tau}_{\mathcal{B}/\mathcal{P}_2}(\boldsymbol{\theta}_{\mathcal{A}_{0,2}/\mathcal{A}_2}(t)) \cdot \frac{\partial \boldsymbol{\omega}_{\mathcal{A}_{0,2}/\mathcal{A}_2}(\boldsymbol{\theta}_{\mathcal{A}_{0,2}/\mathcal{A}_2}(t))}{\partial \dot{q}_j} \\
&- \boldsymbol{F}_{\mathcal{P}_3/\mathcal{P}_1}(\boldsymbol{\delta}_{\mathcal{A}_{0,3,1}/\mathcal{A}_{3,1}}(t)) \cdot \frac{\partial \boldsymbol{\delta}_{\mathcal{A}_{0,3,1}/\mathcal{A}_{3,1}}(t)}{\partial q_j} \\
&- \boldsymbol{\tau}_{\mathcal{P}_3/\mathcal{P}_1}(\boldsymbol{\theta}_{\mathcal{A}_{0,3,1}/\mathcal{A}_{3,1}}(t)) \cdot \frac{\partial \boldsymbol{\omega}_{\mathcal{A}_{0,3,1}/\mathcal{A}_{3,1}}(\boldsymbol{\theta}_{\mathcal{A}_{0,3,1}/\mathcal{A}_{3,1}}(t))}{\partial \dot{q}_j} \\
&- \boldsymbol{F}_{\mathcal{P}_3/\mathcal{P}_2}(\boldsymbol{\delta}_{\mathcal{A}_{0,3,2}/\mathcal{A}_{3,2}}(t)) \cdot \frac{\partial \boldsymbol{\delta}_{\mathcal{A}_{0,3,2}/\mathcal{A}_{3,2}}(t)}{\partial q_j} \\
&- \boldsymbol{\tau}_{\mathcal{P}_3/\mathcal{P}_2}(\boldsymbol{\theta}_{\mathcal{A}_{0,3,2}/\mathcal{A}_{3,2}}(t)) \cdot \frac{\partial \boldsymbol{\omega}_{\mathcal{A}_{0,3,2}/\mathcal{A}_{3,2}}(\boldsymbol{\theta}_{\mathcal{A}_{0,3,2}/\mathcal{A}_{3,2}}(t))}{\partial \dot{q}_j}
\end{aligned} \tag{22}$$

Where the forces and torques are functions of the displacements at the hinge indicated in the subscripts. As with the one panel simulation, these forces and torques are tested as simple linear spring functions as defined in Equation 15. The equations of motion of this system can now be generated using Equations 16 and 22 in Equation 1. This results in a system of 24 equations for the 24 generalized coordinates selected.

THREE PANEL MODEL INITIALIZATION AND VALIDATION

The spacecraft bus and rigid panel mass and inertia properties, position and orientation parameters, and initial conditions are generated here for a multiple panel model in Table 4, Table 5, Table 6, and Table 7, respectively. These parameters represent a simple toy case that is designed to test performance across the generalized coordinates. The results of the 3 panel case simulation run are shown in Figure 6.

Table 4. Model parameters of the single panel simulation check, mass is in kg and inertia is in (kg/m^2) and shows the principle inertias.

m_B	m_{P_1}	m_{P_2}	m_{P_3}	I_B	I_{P_1}	I_{P_2}	I_{P_3}
100	7	7	9	$[100, 100, 100]$	$[1, 1, 0.1]$	$[1, 1, 0.1]$	$[1, 1, 0.1]$

Table 5. Relative positions (m) of the single panel simulation check.

$\boldsymbol{r}_{\mathcal{A}_{0,1}/\mathcal{B}}$	$\boldsymbol{r}_{\mathcal{A}_{0,2}/\mathcal{B}}$	$\boldsymbol{r}_{\mathcal{P}_1/\mathcal{A}_1}$	$\boldsymbol{r}_{\mathcal{P}_2/\mathcal{A}_2}$	$\boldsymbol{r}_{\mathcal{P}_1/\mathcal{A}_{3,1}}$	$\boldsymbol{r}_{\mathcal{P}_2/\mathcal{A}_{3,2}}$
$[0.75, 0.433, 0]$	$[-0.75, -0.433, 0]$	$[1, 1, 0]$	$[1, 1, 0]$	$[1, 1, 0]$	$[1, 1, 0]$

Table 6. Relative orientations (deg) of the single panel simulation check.

$\boldsymbol{\theta}_{\mathcal{A}_{0,1}/\mathcal{B}}$	$\boldsymbol{\theta}_{\mathcal{A}_{0,2}/\mathcal{B}}$	$\boldsymbol{\theta}_{\mathcal{P}_1/\mathcal{A}_1}$	$\boldsymbol{\theta}_{\mathcal{P}_2/\mathcal{A}_2}$	$\boldsymbol{\theta}_{\mathcal{P}_1/\mathcal{A}_{3,1}}$	$\boldsymbol{\theta}_{\mathcal{P}_2/\mathcal{A}_{3,2}}$
$[0, 0, 30]$	$[0, 0, -30]$	$[0, 0, 0]$	$[0, 0, 0]$	$[0, 0, 45]$	$[0, 0, 45]$

CONCLUSION AND FUTURE WORK

Implementation of deployment actuating hinge behavior as internal forces and torques in a multi-body system is demonstrated for a single panel case and a multi-panel case with panel interconnections. The conservation of momentum and conservation of motion validates the derivation and modeling methods. However, the analysis provided in this work is only the first step towards creating realistic models of complex folded deployable structure deployment dynamics. Future work will investigate expanding to complete flasher panel sets and modeling multiple panel interconnections across the system. Additionally, future work will investigate using empirical data to fit force and torque functions that accurately model true hinge behaviors. Flexible high strain composite materials will be tested and an approximate mathematical fit will be pursued. Alternatively, a lookup table of force and torque responses for a range of motions may be generated and interpolated to determine the response at a given configuration. Future systems with a greater number of interconnected bodies may need the assistance of fast multi-body physics software to aid in behavior simulation, where complex behaviors such as contact forces may be studied as well. Integrating the internal hinge force and torque models into these software packages will also be investigated in future work.

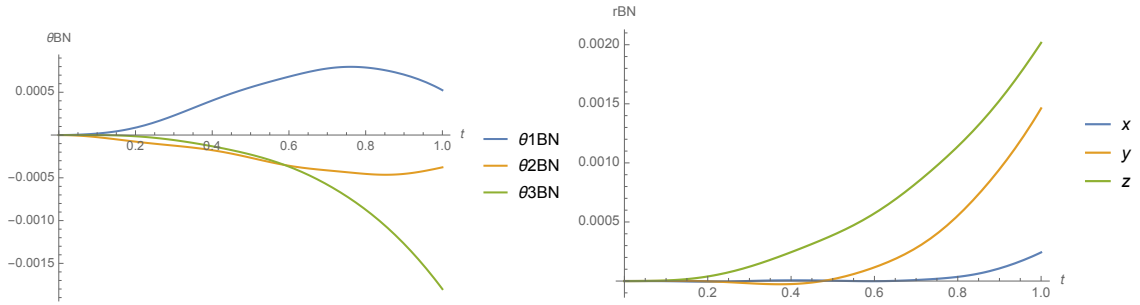

(a) Bus Orientation

(b) B Frame Bus Position

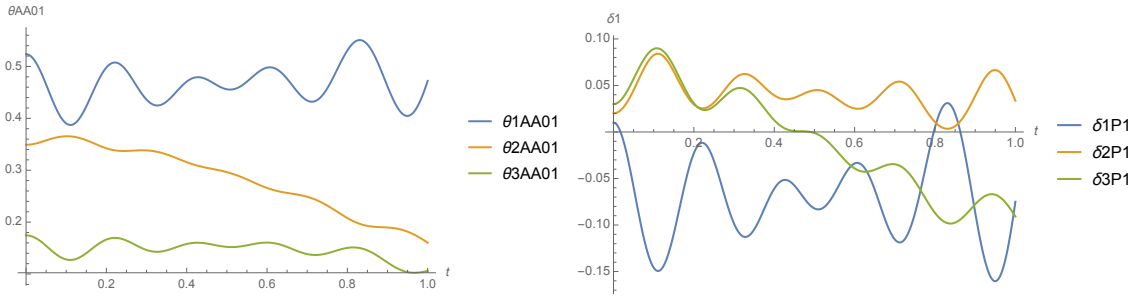

(c) Panel 1 Orientation

(d) Panel 1 Displacement

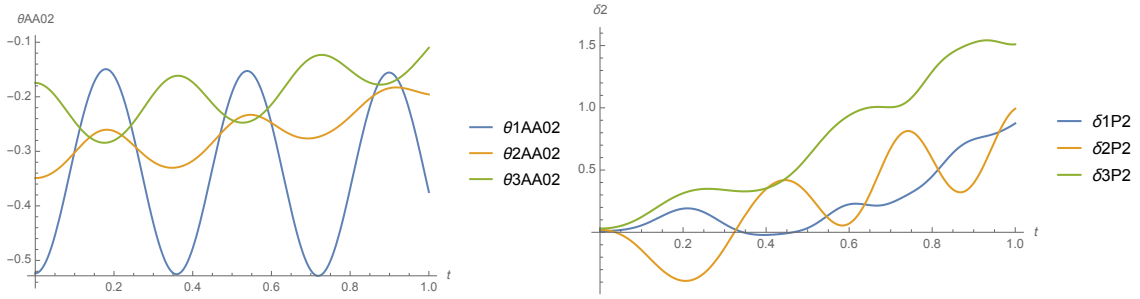

(e) Panel 2 Orientation

(f) Panel 2 Displacement

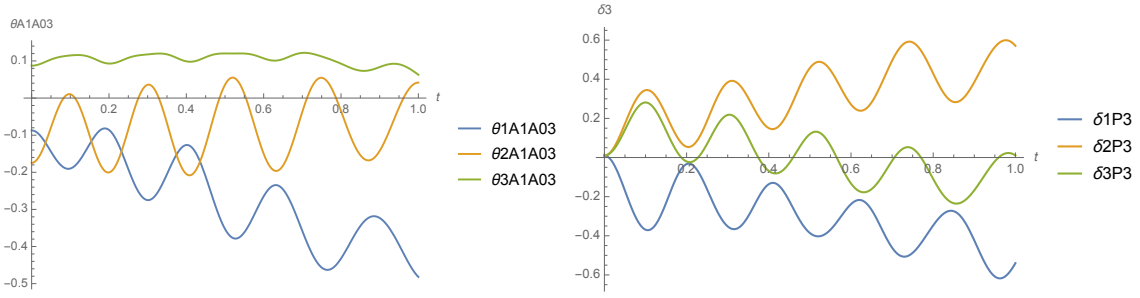

(g) Panel 3 Orientation

(h) Panel 3 Displacement

Figure 6. Three panel simulation results.

Table 7. Initial conditions of the single panel simulation check.

$\boldsymbol{R}_{\mathcal{B}/\mathcal{N}}(0)$	$\boldsymbol{\delta}_{\mathcal{A}_1/\mathcal{A}_{0,1}}(0)$	$\boldsymbol{\delta}_{\mathcal{A}_2/\mathcal{A}_{0,2}}(0)$	$\boldsymbol{\delta}_{\mathcal{A}_{0,3,1}/\mathcal{A}_{3,1}}(0)$
$\mathbf{0}$	$[0.01, 0.02, 0.03]$	$[0.01, 0.02, 0.03]$	$[0.01, 0.01, 0.01]$
$\boldsymbol{\theta}_{\mathcal{B}/\mathcal{N}}(0)$	$\boldsymbol{\theta}_{\mathcal{A}_1/\mathcal{A}_{0,1}}(0)$	$\boldsymbol{\theta}_{\mathcal{A}_2/\mathcal{A}_{0,2}}(0)$	$\boldsymbol{\theta}_{\mathcal{A}_{0,3,1}/\mathcal{A}_{3,1}}(0)$
$\mathbf{0}$	$[30, 20, 10]$	$[-30, -20, -10]$	$[-5, -10, 5]$

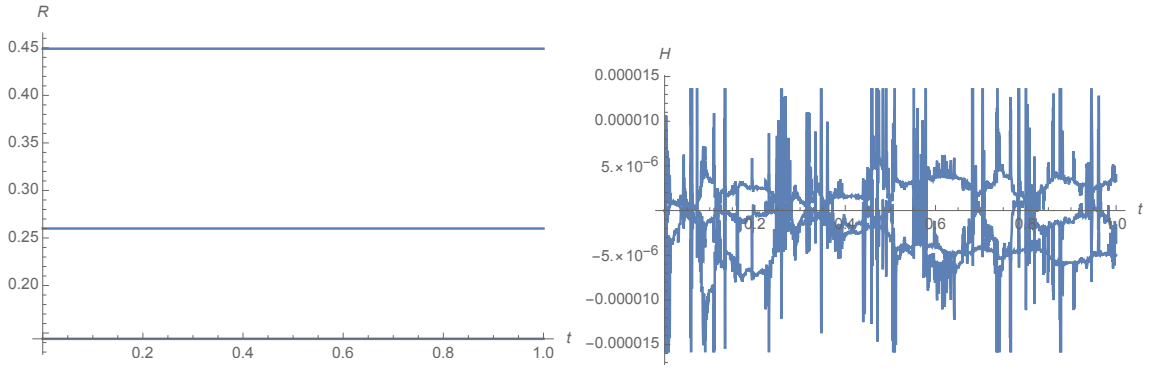

(a) System Barycenter (b) Angular Momentum

Figure 7. Three panel simulation validations.

REFERENCES

[1] J. Banik, *Frontiers of Engineering: Reports on Leading-Edge Engineering from the 2015 Symposium*, ch. Realizing Large Structures in Space. the National Academies Press, 2015.

[2] M. Thomson, D. Lisman, R. Helms, P. Walkemeyer, A. Kissil, O. Polanco, and S.-C. Lee, "Starshade Design for Occulter Based Exoplanet Missions," *Space Telescopes and Instrumentation 2010: Optical, Infrared, and Millimeter Wave*, 2010.

[3] D. Webb, B. Hirsch, V. Bach, J. Sauder, C. Bradford, and M. Thomson, "Starshade Mechanical Architecture and Technology Effort," *3rd AIAA Spacecraft Structures Conference*, 2016.

[4] L. Puig, A. Barton, and N. Rando, "A review on large deployable structures for astrophysics missions," *Acta Astronautica*, 2010.

[5] S. Guest and S. Pellegrino, "Inextensional Wrapping of Flat Membranes," *Proceedings of the First International Seminar on Structural Morphology*, 1992.

[6] T. Nojima, "Origami Modeling of Functional Structures based on Organic Patterns," Master's thesis, Graduate School of Kyoto University, Kyoto, Japan, 2002.

[7] H. Sakamoto, M. C. Natori, S. Kadonishi, Y. Satou, Y. Shirasawa, N. Okuizumi, O. Mori, H. Furuya, and M. Okuma, "Folding patterns of planar gossamer space structures consisting of membranes and booms Hiraku," *Acta Astronautica*, Vol. 94, 2014, pp. 34–41.

[8] M. C. Natori, H. Sakamoto, N. Katsumata, H. Yamakawa, and N. Kishimoto, "Conceptual model study using origami for membrane space structures – a perspective of origami-based engineering," *Mechanical Engineering Reviews*, Vol. 2, No. 1, 2015, pp. 1–15.

[9] J. A. Banik, T. W. Murphey, and H.-P. Dumm, "Synchronous Deployed Solar Sail Concept Demonstration," *49th AIAA/ASME/ASCE/AHS/ASC Structures, Structural Dynamics, and Materials*, Schaumburg, IL, April 2008.

[10] H. Furuya, O. Mori, N. Okuizumi, Y. Shirasawa, M. C. Natori, Y. Miyazaki, and S. Matanaga, "Manufacturing and Folding of Solar Sail 'IKAROS'," *52nd AIAA/ASME/ASCE/AHS/ASC Structures, Structural Dynamics and Materials Conference*, 2011.

[11] W. D. Reynolds and T. W. Murphey, "Elastic Spiral Folding for Flat Membrane Apertures," *Spacecraft Structures Conference*, 2014.

[12] D. Kling, S. Jeon, and J. Banik, "Novel Folding Methods for Deterministic Deployment of Common Space Structures," *3rd AIAA Spacecraft Structures Conference*, 2016.

[13] J. Morgan, S. P. Magleby, and L. L. Howell, "An Approach to Designing Origami-Adapted Aerospace Mechanisms," *Journal of Mechanical Design*, Vol. 138, March 2016, pp. 052301–052311.

[14] H. Sakamoto, Y. Shirasawa, D. Haraguchi, H. Sawada, and O. Mori, "A Spin-up Control Scheme for Contingency Deployment of the Sailcraft IKAROS," *52nd AIAA/ASME/ASCE/AHS/ASC Structures, Structural Dynamics, and Materials Conference*, 2011.

[15] T. W. Murphey, M. E. Peterson, and M. M. Grigoriev, "Four Point Bending of Thin Unidirectional Composite Laminas," *54th AIAA/ASME/ASCE/AHS/ASC Structures, Structural Dynamics, and Materials Conference*, Boston, Massachusetts, April 2013.

[16] S. J. I. Walker and G. Aglietti, "Study of the Dynamics of Three-Dimensional Tape Spring Folds," *AIAA Journal*, Vol. 42, April 2004, pp. 850–856.

[17] H. Schaub and J. L. Junkins, *Analytical Mechanics of Space Systems*. 1801 Alexander Bell Drive, Reston, Virginia, 20191-4344: American Institute of Aeronautics and Astronautics, Inc., 3rd ed., 2014.

[18] T. R. Kane and D. A. Levinson, *Dynamics: Theory and Applications*. New York: McGraw-Hill, Inc., 1985.